Aquaculture 530 (2021) 735781

Contents lists available at ScienceDirect

Aquaculture

journal homepage: www.elsevier.com/locate/aquaculture

# QTL mapping for orange shell color and sex in the Pacific oyster (*Crassostrea gigas*)

Ziqiang Han[a], Qi Li[a,b,*], Chengxun Xu[a], Shikai Liu[a], Hong Yu[a], Lingfeng Kong[a]

[a] Key Laboratory of Mariculture, Ministry of Education, Ocean University of China, Qingdao 266003, China
[b] Laboratory for Marine Fisheries Science and Food Production Processes, Qingdao National Laboratory for Marine Science and Technology, Qingdao 266237, China

ARTICLE INFO

*Keywords:*
*Crassostrea gigas*
Shell color
Sex
QTL mapping
F2 population

ABSTRACT

Molluscan shellfish have a diverse form of shell coloration and sex determination, understanding the genetic mechanism under these two traits is crucial to their germplasm exploitation and conservation. In our breeding program, a novel orange-shell variant of *C. gigas* was obtained, and an F2 family was constructed by crossing an orange-shell male with a black-shell female. This F2 family provided an ideal material for QTL mapping of orange shell color and sex traits of *C. gigas* simultaneously. Here, a high-density genetic linkage map containing 1799 SNP markers was constructed using this F2 family by genotyping-by-sequencing. These markers were distributed on 10 linkage groups and the total map size was 828.31 cM, with an average marker interval of 0.58 cM. Based on this map, six chromosome-level significant QTLs associated with orange shell color were detected, with the phenotypic variance explained ranging from 9.10% to 12.30%. Within the QTL regions, four candidate genes, 3-ketoacyl-CoA thiolase A, fibroblast growth factor receptor 4, poly [ADP-ribose] polymerase tankyrase-1 and tripartite motif-containing protein 45-like, related to the organic matrix of mollusk shells or collagen were identified. Additionally, only one genome-wide significant sex-related QTL was detected, which explained 19.30% of phenotypic variance. Two sex-related genes, proteasome subunit beta type-3 and G-protein coupled estrogen receptor 1 were identified within the QTL region. The QTLs and candidate genes identified in this study provide valuable resources for further investigations on the molecular mechanisms of shell color and sex in *C. gigas*.

## 1. Introduction

The phylum Mollusca is the largest phylum in the marine realm, and the vast majority of them are shelled. The diverse and fabulous colors and patterns of molluscan shells have attracted many collectors and scientists for hundreds of years (Williams, 2017). Similar to its remarkable various shell coloration, molluscs also showed a wide variety of sexual systems, ranging from dioecy to simultaneous hermaphroditism and sequential hermaphroditism (Breton et al., 2018). Thus, identifying genomic regions associated with sex determination and shell coloration in molluscs has always been a research topic of great interest. Considering the molluscan shellfish production is an important source of protein for human and their substantial potential for genetic improvement (Gjedrem and Rye, 2018), a better understanding of the genetic mechanisms underlying these two traits is crucial to their germplasm exploitation and conservation.

The Pacific oyster, *Crassostrea gigas*, is one of the most important commercial molluscs. Meanwhile, *C. gigas* is also a typical organism to understand the molluscan sex determination, since it lacks heteromorphic sex chromosomes and exhibits a unique and complex sexual system characterized by protandry, sex change (sequential hermaphroditism), and rare simultaneous hermaphroditism (Broquard et al., 2020; Yasuoka and Yusa, 2016). Although the sex determination of *C. gigas* can be affected by environmental factors such as temperature and food availability (Santerre et al., 2013), the importance of genetic factors has also been suggested through the analysis of family sex ratios and a single major gene with 2 or 3 genotypes models were proposed (Hedrick and Hedgecock, 2010; Guo et al., 1998). Although one QTL associated with sex was detected in *C. gigas* by a linkage map constructed with SSR and AFLP markers (Guo et al., 2012), whether the sex is genetically determined, and whether it is controlled by a dominant gene or multiple genes is still controversial (Hedrick and Hedgecock, 2010; Yue et al., 2018; Zhang et al., 2014). Detailed examination of experimental crosses using a large number of markers should help to understand the genetic basis of sex determination of *C. gigas*.

Shell color of *C. gigas* exhibits a continuous variation in nature,

* Corresponding author at: Key Laboratory of Mariculture, Ministry of Education, Ocean University of China, Qingdao 266003, China.
*E-mail address:* qili66@ouc.edu.cn (Q. Li).

https://doi.org/10.1016/j.aquaculture.2020.735781
Received 15 June 2020; Received in revised form 27 July 2020; Accepted 28 July 2020
Available online 06 August 2020
0044-8486/ 

ranging from near-white (pigment-free) to near-black (full pigmented), and mixed with some golden and purple (Brake et al., 2004; Ge et al., 2015). Although phenotype results of families indicate that the shell color of *C. gigas* is genetically determined (Brake et al., 2004), the diversity and irregularity of shell color in natural population make it difficult to analyze the underlying genetic mechanism. Notably, shell pigmentations of *C. gigas* show medium to high heritability (Evans et al., 2009; Wan et al., 2017; Xu et al., 2017), and three lines with solid black, white and golden shell color in *C. gigas* have been obtained through artificial selection (Ge et al., 2015; Xu et al., 2019). Based on these solid shell color lines, the inheritance patterns of black and golden shell colors have been investigated (Ge et al., 2015; Xu et al., 2019), and the QTLs associated to these two shell colors were identified, through two F1 linkage maps that were constructed with a small number of EST-SNP or SSR, respectively (Song et al., 2018; Wang et al., 2018). Given the complexity and variety of shell pigmentation in *C. gigas*, it is critical to study the formation mechanism of more other colors to better understand its genetic basis. In our previous work of family breeding, a novel shell color variant of *C. gigas* was obtained with both shells being orange color (Han and Li, 2018; Han et al., 2019). Unlike the inheritance pattern of the golden shell color that is dominant over the white and has an epistatic effect on the black pigmentation (Ge et al., 2015), the orange shell color is a recessive trait compared to black and white, and the genetic locus controlling the orange has no effect on the black locus (Han and Li, 2020). Thus, study on the formation mechanism of the orange shell variant is expected to bring new discoveries to the genetic basis of shell pigmentation in *C. gigas*.

Quantitative trait locus (QTL) mapping, as a basic method to localize genetic determinants of phenotypes, provides powerful tool to investigate the underlying mechanisms of important traits. Compared with genetic maps constructed with a small number of AFLP, SSR or SNP, high-density genetic maps greatly increase the marker density and improve the accuracy of QTL mapping. With the advancement of next-generation sequencing technology, high-density genetic maps have applied in many aquaculture species. In *C. gigas*, three high-genetic maps have been reported, but only for QTL mapping of growth and nutritional traits (Hedgecock et al., 2015; Li et al., 2018; Wang et al., 2016). In our previous study (Han and Li, 2020), an F2 family was generated by crossing orange and black shell oysters (Fig. 1a), which is an ideal population for QTL mapping of shell color and sex traits of *C. gigas* simultaneously. In this study, a high-density genetic map was constructed with this F2 family, with the objective to map the QTLs associated with orange shell color and sex of *C. gigas*.

## 2. Methods and materials

### 2.1. Mapping population

Oysters from the orange shell line and black shell line of *C. gigas* were used as parents in this study. The black shell line was initiated in 2010, based on relatively black shell oysters collected from wild populations of *C. gigas* in Rushan, Shandong Province, China (36.5° N, 121.4° E). Selective breeding for solid black shell and fast-growing traits were implemented through four generations of family selection and subsequent three generations of mass selection (Xu et al., 2017). The orange shell line was established based on four oysters (two females and two males) with left and right orange shells. These four orange shell oysters were unexpectedly identified in the offspring of purple-black shell oysters, which were originally produced by crossing females with solid black left shell and males with solid purple left shell collected from the cultured populations of *C. gigas* in Rushan (Han et al., 2019). Later, three generations of family selection and subsequent three generations of mass selection were used to fix the orange shell and enhance the growth performance of orange shell line (Han and Li, 2020). In both lines, no other shell color phenotype was observed; thus, oysters are expected to be homozygous at shell color loci. In July 2017, a female with solid black shell and a male with solid orange shell selected from their respective lines were crossed to produce the first-generation (F1) family. In June 2018, three females and three males were randomly selected from the F1 family and mated to construct three second-generation (F2) families (Fig. 1a) (Han and Li, 2020). From these three F2 families, family 0618–25 with 180 black oysters and 53 orange oysters (3:1, chi-squared test: $P > .05$) was selected as the mapping family, because it has the largest number of oysters. A total of 90 oysters with black shell and 30 oysters with orange shell were randomly selected from family 0618–25 at 12 months old as the mapping population. All samples were shucked and their muscles were stored at −30 °C for DNA extraction, and then their shells were cleaned and air-dried in dark.

### 2.2. Phenotyping

The sex of each progeny was identified by dissection and microscopic examination of the gonad. The shell color is described by two methods: firstly, shell color was analyzed as a binary trait, and oysters were classified into orange or black by eye observation according to the phenotypes of two parents; secondly, shell color was analyzed as a quantitative trait, and the left and right shells were quantified by a computerized image acquisition and analysis protocol, respectively, as described in Wan et al. (2017). Photos were taken in a small studio (60 cm × 60 cm × 60 cm), with two LED light panels (illumination: 1000 LUX; length: 60 cm) located at the top 20 cm and 40 cm respectively. To capture image, shells were placed on a matte blue background, and a camera (Nikon D4) was fixed vertically 35 cm above the shells. The camera was set as follows: manual model, no flash, no zoom, shutter speed: 1/160, lens aperture: 5.6, ISO: 200, resolution: 5184 × 3456 pixels and images were saved in JPEP format in RGB color coordinates. The camera was connected to a computer by USB interface, and the shooting was controlled in the computer. The image was analyzed with Photoshop CS6 software to obtain the mean R (0–225), G (0–225) and B (0–225) values of the coloring area of these shells. H (hub), S (saturation) and V (brightness or value) values were transferred from these R, G and B values, respectively with an online software program (www.colorizer.org at http://colorizer.org/). HSV color space gives values closer to human vision than RGB model (Stenger et al., 2019). The HSV color space can be visualized as an inverted cone for illustrating the relationship of hue, saturation and brightness (Hoang et al., 2017). Hue was expressed as the degrees (0–360) around the cone, in which the zero indicate red, 120 indicate green, and 240 indicate blue. Saturation expressed as the distance to the axis ranged from 0% (no color) to 100% (intense color). Brightness (or value) expressed as the altitude of the cone and ranged from 0% (is always black; depending on the saturation,) to 100% (may be white or a more or less saturated color). The actual value of hub is record as H′, and the H that used in analyses was transformed from H′ according to the following formula: if $H' > 180$, then $H = H' - 180$; if $H' < 180$, then $H = H' + 180$. To ensure the accuracy of phenotype collection, some individuals with severely contaminated shell surface were replaced with missing values.

### 2.3. GBS library preparation, sequencing and genotyping

Genomic DNA of 120 F2 progeny and two grandparents ($P_O$ and $P_B$) was extracted from muscle tissue using a standard phenol-chloroform method (Sambrook and Russell, 2001). GBS (genotype-by-sequencing) libraries were constructed according to the protocol described in (Elshire et al., 2011; Sonah et al., 2013). Briefly, genomic DNA was digested by double restriction enzyme *Eco*RI and *Hae*II (New England Biolabs, NEB), followed by ligation with barcoded adapters for individual labeling. Next, each sample was amplified in multiplex, and 375–400 bp fragments (with index and adaptors) were isolated by a Gel Extraction Kit (Qiagen). These fragments were then purified using

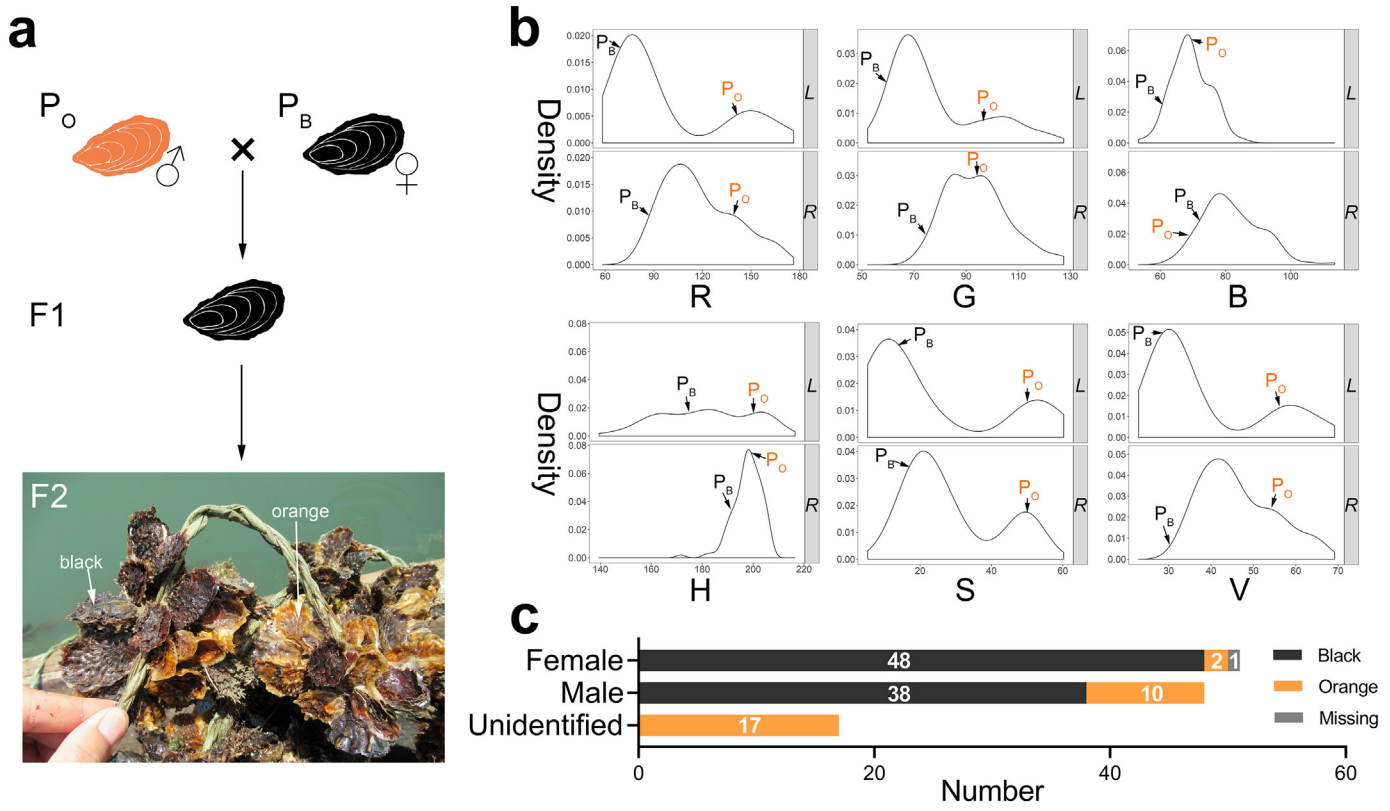


**Fig. 1.** Representative F2 mapping population of the Pacific oyster at 3 months age ($P_O$, parent with orange-shell, $P_B$, parent with blank-shell) (a), Density plot of quantified results of the left and right shell coloration of the F2 mapping population by RGB and HSV models (R, red, G, green, B, blue, H, hue, S, saturation and V, value) (b), and the distribution of orange and black oysters of females and males in the F2 mapping population (oysters were classified into orange or black by eye observation according to the phenotypes of two parents) (c). (For interpretation of the references to color in this figure legend, the reader is referred to the web version of this article.)

Agencourt AMPure XP (Beckman), and used for Paired-End 150 sequencing on Illumina HiSep™ platform. All raw reads were deposited in the NCBI Sequence Read Archive (SRA) database (accession no. PRJNA646858).

The sequences of each sample were separated based on their individual barcodes. Raw reads were fist filtered to clean reads by using fastp (Chen et al., 2018), and then FastQC (http://www.bioinformatics.babraham.ac.uk/projects/fastqc/) was used to check the quality of clean reads. Secondly, clean reads of each sample were aligned to the Pacific oyster reference genome (cgigas_uk_roslin_v1, GCA_902806645.1) using BWA (Burrows-Wheeler Aligner) mem parameter (Li and Durbin, 2009). Thirdly, duplicate reads were marked and removed using MarkDuplicates of Picard (http://broadinstitute.github.io/picard/). Next, pstacks, cstacks, sstacks, and genotype procedure of Stacks 1.48 software (Catchen et al., 2013) were used in turn to generate mappable markers. The pstacks module was used to build loci, in which the minimal reads depth for parents were 8, and for progeny were 5. In the cstacks module, two mismatches allowed between sample loci when build the catalog, followed by sstacks using default parameters. The genotype module was then used to genotype each locus, in which the map type was set as F2, the minimum coverage to report a stack was set as 5, and missing value rate for each locus less than 20%.

### 2.4. Linkage map construction

A linkage map was constructed with JoinMap 4.0 (Van Ooijen, 2006) using markers in the aa × bb type. Makers showing segregation distortion (chi-squared test, $x^2 > 30$) and individuals with missing date larger than 25% were excluded for the linkage map construction. Markers were assigned into linkage groups (LG) with LOD = 18 and each linkage group has no less than 10 markers. Regression mapping algorithm of JoinMap was used to order makers within each LG, and then Kosambi's was used to calculated the marker distance. Mapchart 2.3 (Voorrips, 2002) was used to draw the final linkage map. Linkage groups were named in Arabic numerals according to the chromosome order of the Pacific oyster reference genome (cgigas_uk_roslin_v1).

### 2.5. QTL identification

MapQTL 6.0 (Van Ooijen, 2009) was used to detect QTLs for all analyzed traits, with the mapping step size was set to 0.5 cM. The LOD threshold for each trait was determined by permutation test ($n = 1000$, $P < .05$) on genome level and each LG level, respectively. For each trait, the interval mapping was first used to reveal candidate QTL interval, and then the loci with largest LOD scores were treated as cofactors. Next, multiple QTL mapping was used to detect QTLs, and LOD peaks higher than the LOD threshold was identified as QTLs. The CI was determined based on the location of LOD peak and surrounding region. When a QTL was mapped to a single marker, the position of the QTL was represented by the location of this marker. To identify the potential candidate genes related to sex or shell pigmentation around these markers, the 250 kb of both flanking regions around the nearest marker to the peak LOD were scanned based on the *C. gigas* reference genome (cgigas_uk_roslin_v1), and candidate genes were annotated by *C. gigas* gene annotation database (NCBI Annotation Release: 102).

**Table 1**
Descriptive statistics for the shell color parameters (RGB and HSV models) of the parents and F2 mapping population.

| Trait[a] | Parents[b] | | F2 mapping population | | |
|---|---|---|---|---|---|
| | $P_B$ | $P_O$ | Mean ± SD | Range | CV (%)[c] |
| Left-R | 68.04 | 140.58 | 96.81 ± 34.13 | 58.28–176.32 | 35.26 |
| Left-G | 59.9 | 94.77 | 77.54 ± 17.31 | 52.13–123.78 | 22.32 |
| Left-B | 60.92 | 69.46 | 69.37 ± 5.89 | 53.36–85.80 | 8.5 |
| Left-H | 173.07 | 201.35 | 181.43 ± 18.02 | 139.48–216.49 | 9.93 |
| Left-S | 11.8 | 50.6 | 22.97 ± 18.42 | 5.27–60.23 | 80.2 |
| Left-V | 26.68 | 55.13 | 37.97 ± 13.39 | 22.85–69.15 | 35.26 |
| Right-R | 86.57 | 139.15 | 117.96 ± 22.2 | 83.07–169.74 | 18.82 |
| Right-G | 75.57 | 93.56 | 94.14 ± 12.14 | 72.07–127.46 | 12.89 |
| Right-B | 73.45 | 67.21 | 81.84 ± 9.02 | 63.59–113.43 | 11.02 |
| Right-H | 189.7 | 201.98 | 197.67 ± 5.65 | 171.50–206.20 | 2.86 |
| Right-S | 15.2 | 51.7 | 28.60 ± 13.08 | 9.08–54.70 | 45.75 |
| Right-V | 33.95 | 54.47 | 46.26 ± 8.71 | 32.58–66.56 | 18.83 |

[a] Left, left shell, right, right shell; R, red, G, green, B, blue, H, hue, S, saturation and V, value.
[b] $P_O$, parent with orange-shell, $P_B$, parent with blank-shell.
[c] CV = variation coefficient.

## 3. Results

### 3.1. Sex and shell color traits

Sex was considered as a binary trait, and a total of 51 females and 48 males were identified in 116 progenies, in addition 17 unidentified individuals (Fig. 1c). shell color was described by two methods. Firstly, shell color was considered as a binary trait, and 86 black, 29 orange and 1 missing were identified (Fig. 1c). Secondly, shell color of left and right valves was quantified by RGB and HSV models, respectively. The variation coefficient (CV) of the left shell is larger than that of the right shell in R, G, H, S and V values (Table 1). For left shells, the density of R, G, S and V values showed bimodal distribution patterns, and the two parental values were close to different peaks, respectively; whereas B and H values showed normal distribution patterns (Fig. 1b). For right shells, only the density of S values showed bimodal distribution pattern, and the parental values were close to different peaks, respectively; whereas the rest five values were all normal distributed, of which the parental values differ greatly in R and V values (Fig. 1b).

### 3.2. Linkage map

After quality control, a total 440.47 million clean reads were obtained for further analysis, including 7.05 million reads for the female parent, 7.11 million clean reads for the male parent, and an average of 3.55 million reads per progeny. By removing reads with a sequencing depth less than 8 in the parents and 5 in the progenies, the average sequencing depth of the loci of the two parents were 14.61 and 15.49, respectively, and the average depth of the progenies ranged from 7.88 to 12.09. Further, by making the missing rate of each genotype less than 20% and the genotype missing rate of each progeny less than 25% (116 progenies passed the screening), a total of 3959 markers were screened, including 2497 aa × bb. After discarding the markers showing segregation distortion (chi-squared test, $\chi^2 > 30$), the remaining of 1850 makers were used for the linkage map assignment.

A total of 1799 markers, including 1748 unique markers, were assigned into 10 linkage groups (LGs), of which LG7 has a maximum of 294 markers and LG5 has a minimum of 68 markers (Fig. 2 and Table 2). The linkage map spanned 828.31 cM with an average marker interval of 0.58 cM (Table 2). The length of each linkage groups ranged from 62.93 to 114.39 cM with an average of 82.83 cM. The detail of each marker was presented in Supplementary Table S1.

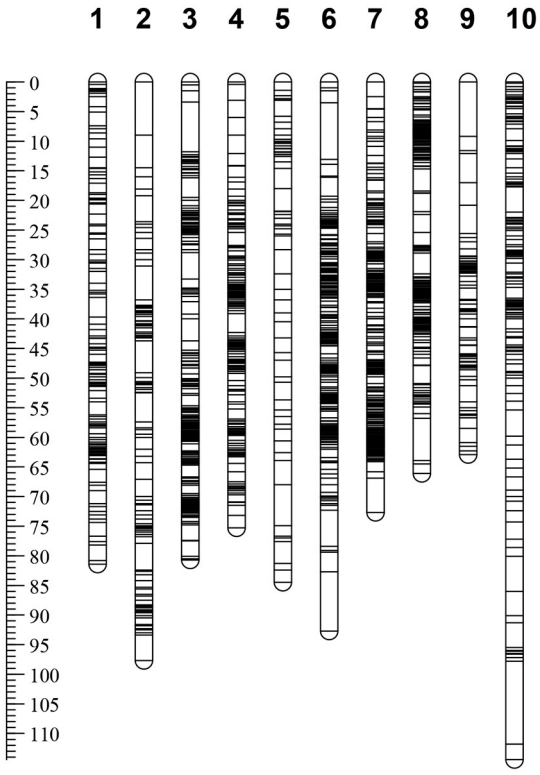


**Fig. 2.** High-density genetic linkage map for the Pacific oyster.

**Table 2**
Basic information of genetic linkage map of the Pacific oyster.

| LG | No. markers | No. SNPs | Length (cM) | Marker interval | No. unique loci[a] | Average interval of unique loci[b] |
|---|---|---|---|---|---|---|
| 1 | 135 | 289 | 81.42 | 0.61 | 132 | 0.62 |
| 2 | 110 | 273 | 97.71 | 0.9 | 107 | 0.92 |
| 3 | 262 | 548 | 80.68 | 0.31 | 254 | 0.32 |
| 4 | 192 | 444 | 75.25 | 0.39 | 186 | 0.41 |
| 5 | 68 | 157 | 84.45 | 1.26 | 65 | 1.32 |
| 6 | 264 | 570 | 92.67 | 0.35 | 255 | 0.36 |
| 7 | 294 | 642 | 72.68 | 0.25 | 286 | 0.26 |
| 8 | 222 | 580 | 66.13 | 0.3 | 218 | 0.30 |
| 9 | 84 | 214 | 62.93 | 0.76 | 83 | 0.77 |
| 10 | 168 | 340 | 114.39 | 0.68 | 162 | 0.71 |
| Sum | 1799 | 4057 | 828.31 | – | 1748 | – |
| Mean | 179.9 | – | 82.83 | 0.58 | 174.8 | 0.6 |

[a] Number of loci occupying different positions on the map.
[b] Average interval of loci occupying different positions on the map.

### 3.3. QTL mapping and potential candidate gene detection

A total of seven QTLs were identified on LG2 and LG9 (Fig. 3a). For sex trait, only one genomic-wide QTL (Sex-1) was detected at LG9, explaining 19.30% phenotypic variation (Table 3 and Fig. 3b). Two genes, including proteasome subunit beta type-3 (LOC105328897) and G-protein coupled estrogen receptor 1 (LOC105338021) were identified around the QTL-linked markers (Table 4).

For thirteen shell color traits, six chromosome-wide significant QTLs were identified for three traits, including binary color (S-color), saturation of left shell (Leftshell-S) and values of left shell (Leftshell-V). However, no QTLs was identified for left shell color described by RGB model and all color traits of right shell. The QTL of S-color is located at 25.64 cM of LG9 and contained only one marker 100,868, contributing to 10.30% of the PVE (Table 3 and Fig. 3c). Three of the four QTLs of

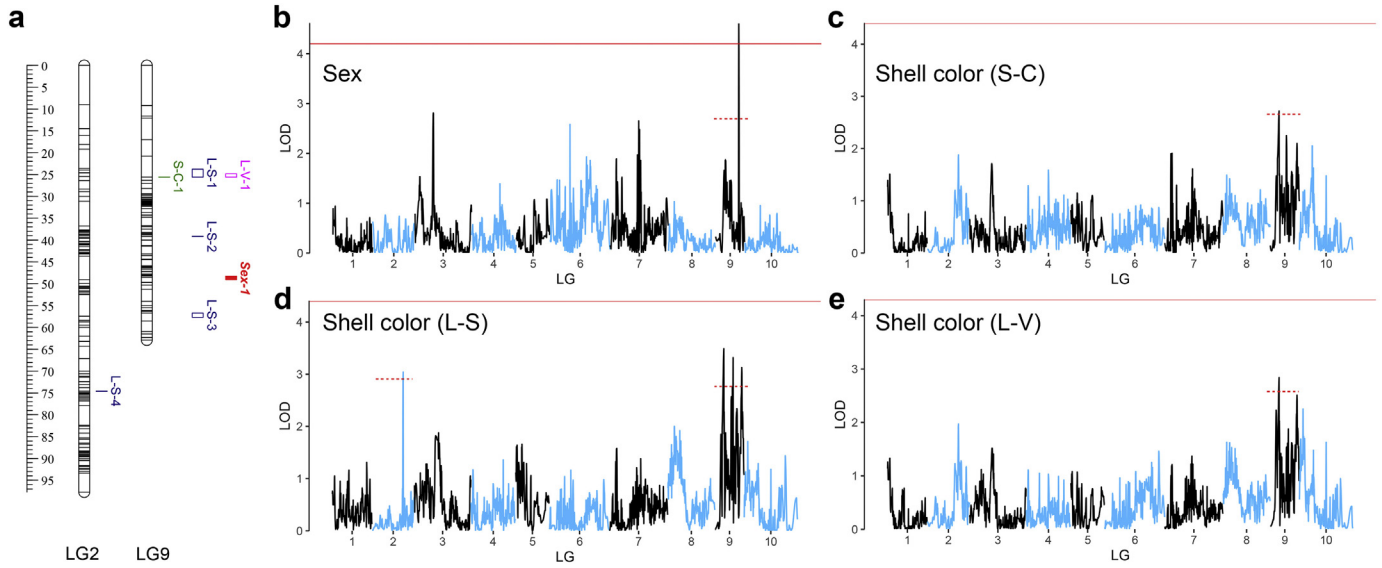


**Fig. 3.** Distribution of QTLs associated with shell color and sex on linkage group 2 and 9 of the Pacific oyster (a), and LOD scores along the 10 linkage groups variations in shell color and sex traits in the Pacific oyster (b, c, d and e). The red dashed and solid lines indicated the chromosome-wide and genome-wide significance thresholds. (For interpretation of the references to color in this figure legend, the reader is referred to the web version of this article.)

**Table 3**
QTLs detected for sex and shell color in the Pacific oyster.

| Traits[a] | QTL | LG | CI (cM) | Peak LOD[b] | PVE (%)[c] | No. of Markers | Nearst marker |
|---|---|---|---|---|---|---|---|
| Sex | Sex-1 | 9 | 48.312–49.132 | 4.61** | 19.30 | 2 | 109,940 |
| S-color | S-C-1 | 9 | 25.64 | 2.72* | 10.30 | 1 | 100,868 |
| Leftshell-S | L-S-1 | 9 | 23.822–25.640 | 3.49* | 12.30 | 1 | 100,868 |
| | L-S-2 | 9 | 39.182 | 3.32* | 10.10 | 1 | 99,429 |
| | L-S-3 | 9 | 56.709–57.709 | 2.97* | 9.10 | 1 | 113,398 |
| | L-S-4 | 2 | 74.598 | 3.04* | 10.60 | 1 | 167,196 |
| Leftshell-V | L-V-1 | 9 | 24.822–25.640 | 2.84* | 11.30 | 1 | 100,868 |

[a] S-color, Binary value; Leftshell-S, Saturation of left shell; Leftshell-V, Values of left shell.
[b] *, chromosome-wide significance; **, genome-wide significance.
[c] PVE, Percentage of phenotypic variance.

Leftshell-S were distributed on LG9, of which the marker 100,868 explained 12.30% phenotypic variation, and the other two markers 99,429 and 113,398 explained 10.10% and 9.10%, respectively, in addition to a marker 167,196 located in LG2 explained 10.60% phenotypic variation (Table 3 and Fig. 3d). For Leftshell-V, only one QTL was detected at marker 100,868 of LG9, contributing to 11.30% of the PVE (Table 3 and Fig. 3e). Five of the six QTLs related shell color were distributed on LG9, and the marker 100,868 was included in the QTLs of these three traits (Fig. 3a). The gene 3-ketoacyl-CoA thiolase A, peroxisomal (LOC105319875) was identified around marker 100,868. Moreover, three genes, including fibroblast growth factor receptor 4 (LOC105346247), poly [ADP-ribose] polymerase tankyrase-1 (LOC105342415) and tripartite motif-containing protein 45-like (LOC117680499) were identified around other QTL-linked markers (Table 4).

## 4. Discussion

### 4.1. Linkage map

High-density genetic linkage map is an important pre-requisite for QTL fine mapping of traits of interest. A high-density genetic map containing 1799 markers was constructed for *C. gigas* by a F2 family (Fig. 2 and Table 2). For *C. gigas,* three high-density maps have been reported (Hedgecock et al., 2015; Li et al., 2018; Wang et al., 2016). The number of markers of our map were higher than the maps constructed by Hedgecock et al. (2015) and Wang et al. (2016), but lower than that of Li et al. (2018). The total length of our map was 828.31 cM, similar to that of previous studies (Hedgecock et al., 2015; Wang et al., 2016). Such a high-density genetic map constructed in this study is helpful to detect QTL associated shell color and sex traits of *C. gigas*.

**Table 4**
Annotation of the QTLs associate with sex and shell color in the Pacific oyster.

| QTL | Marker | Gene | Distance (kb)[a] | Gene annotation |
|---|---|---|---|---|
| Sex-1 | 109,940 | LOC105328897 | 110.76–115.29 | Proteasome subunit beta type-3 |
| | 109,708 | LOC105338021 | 79.62–82.71 | G-protein coupled estrogen receptor 1 |
| S-C-1, L-S-1, L-V-1 | 100,868 | LOC105319875 | 2.27–7.83 | 3-Ketoacyl-CoA thiolase A, peroxisomal |
| L-S-2 | 99,429 | LOC105346247 | 215.29–219.92 | Fibroblast growth factor receptor 4 |
| L-S-3 | 113,398 | LOC105342415 | 217.99–221.10 | Poly [ADP-ribose] polymerase tankyrase-1 |
| L-S-4 | 167,196 | LOC117680499 | 197.74–222.28 | Tripartite motif-containing protein 45-like |

[a] Distances between candidate genes and markers.

### 4.2. The importance of phenotypic description methods

The influence of marker density of genetic map on mapping accuracy has been well documented (Laghari et al., 2014), but the effect of different description methods of phenotypes on mapping results is always ignored in previous studies about QTL mapping of color traits. In these studies, only one description method was used to describe the color trait (Bai et al., 2016; Nie et al., 2017). In this study, both qualitative description by eye observation and quantitative methods based on the image acquisition system were used to describe the shell color trait (Fig. 1 and Table 1). Only one QTL containing marker 100,868 was detected by the binary results resulting from eye observation. However, besides the marker 100,868, other three markers were identified based on these HSV quantitative results (Fig. 3 and Table 3). This result indicates that the quantitative results can provide more information than the qualitative description. For example, the variation in saturation and brightness of a color cannot be reflected by qualitative description. In addition, different quantitative methods also have a great influence on the mapping results. RGB and HSV models were used to quantify the shell color in this study. For the left shell color, however, five QTLs just detected in HSV model, and no QTLs was detected in RGB model. Those results suggested that using a variety of phenotype description methods will help to improve the accuracy of mapping results.

### 4.3. QTL for shell color

Orange-shell *C. gigas* is a novel shell color variant and the molecular mechanism underlying the orange shell remain unknow. In our previous study, the orange shell color is proved to be recessive to black, and may be controlled by two independent loci according to the phenotypic segregate ratio in the F1, F2 and test families of cross between orange and black shell oysters (Han and Li, 2020). One QTL, S-C-1, associated with the orange shell color was detected by the binary results in the present study, but this QTL is chromosome-wide significant and explained only 10.30% of the phenotypic variance in shell color trait (Fig. 3 and Table 3). This suggests that the QTL S-C-1 is not the major loci, but is in linkage disequilibrium with the causal locus that determines the orange shell color. Besides the QTL S-C-1, other four QTLs were detected by saturation values and one QTL was detected by brightness values of left shells, and the percentage of variance explained by these five QTLs ranged from 9.10% to 12.30% (Fig. 3 and Table 3), suggesting that the saturation of left shell is determined by many other loci with small effects.

QTL mapping provides a powerful tool for detecting potential genes with certain physiological functions. All these QTLs for binary results, saturation and brightness of left shell contained the marker 100,868, around which a gene 3-ketoacyl-CoA thiolase A, peroxisomal (LOC105319875) was identified. The 3-ketoacyl-CoA thiolase A, peroxisomal is involved in the pathway of lipid metabolism (Swinkels et al., 1991), which is related to carotenoid accumulation in copepods (Schneider et al., 2016). In addition, fibroblast growth factor receptor 4 (L-S-2) has tyrosine-protein kinase as cell-surface receptor, which plays a role in regulation of lipid metabolism and vitamin D metabolism (Kurosu et al., 2007). Lipid metabolism is related to the accumulation of carotenoid (Schneider et al., 2016), and vitamin D metabolism is associated with skin color in Caucasian populations (Saternus et al., 2015; Slominski et al., 2017). Poly [ADP-ribose] polymerase tankyrase-1 (L-S-3) involved in the Wnt signaling pathway, which is related to the formation of melanocytes (D'Mello et al., 2016), and tripartite motif-containing protein 45-like (L-S-4) is involved in zinc ion binding, which has been reported related to the shell pigmentation in *Mercenaria mercenaria* (Hu et al., 2019) and *Argopecten irradians* (Teng et al., 2018).

### 4.4. QTL for sex

Understanding of the genetic mechanisms for sex determination in *C. gigas* is still limited. High-density genetic linkage map provides useful tool for determining the number and position of the sex-related QTLs. Only one genome-wide significant sex-related QTL was detected and explained 19.30% of the phenotypic variance (Fig. 3 and Table 3). This result consists with QTL result obtained by the linkage map constructed by SSRs and AFLPs in an F1 full-sib family of *C. gigas*, in which one QTL for sex was detected (Guo et al., 2012). Although 19.30% of the phenotypic variance is not enough to support that the sex of *C. gigas* is controlled by a dominant gene (Guo et al., 1998; Hedrick and Hedgecock, 2010), this QTL region would include major genes playing critical roles in sex determination of the *C. gigas*. From the sex-related QTL interval, two candidate genes associated with sex were identified. The proteasome subunit beta type-3 is a component of the 20S core peoteasome complex, which plays an essential role in spermatogenesis (Ben-Nissan and Sharon, 2014), and the G-protein coupled estrogen receptor 1 that binds to 17-beta-estradiol with high affinity, plays a role in reproduction by triggering mitochondrial apoptosis during pachytene spermatocyte differentiation (Sirianni et al., 2008).

## 5. Conclusion

In this study, a high-density genetic linkage map containing 1799 markers was constructed for *C. gigas* using a F2 family. Based on this map, six QTLs associated with the orange shell color were detected for the first time. Moreover, one genome-wide significant sex-related QTL was detected. These QTLs and candidate genes identified provide valuable resources for further investigation on the molecular mechanisms underlying shell color and sex in *C. gigas*, which will be crucial for the germplasm exploitation and conservation of *C. gigas*.

Supplementary data to this article can be found online at https://doi.org/10.1016/j.aquaculture.2020.735781.

## Declaration of Competing Interest

The authors declare no conflict of interest.

## Acknowledgements

This work was supported by the grants from National Natural Science Foundation of China (31972789 and 31802293), Shandong Province (2017LZGC009), Weihai City (2018NS01), and the Ocean University of China-Auburn University Joint Research Center for Aquaculture and Environmental Science.

## References

Bai, Z.Y., Han, X.K., Liu, X.J., Li, Q.Q., Li, J.L., 2016. Construction of a high-density genetic map and QTL mapping for pearl quality-related traits in *Hyriopsis cumingii*. Sci. Rep. 6, 32608. https://doi.org/10.1038/srep32608.

Ben-Nissan, G., Sharon, M., 2014. Regulating the 20S proteasome ubiquitin-independent degradation pathway. Biomolecules 4, 862–884. https://doi.org/10.3390/biom4030862.

Brake, J., Evans, F., Langdon, C., 2004. Evidence for genetic control of pigmentation of shell and mantle edge in selected families of Pacific oysters, *Crassostrea gigas*. Aquaculture 229, 89–98. https://doi.org/10.1016/s0044-8486(03)00325-9.

Breton, S., Capt, C., Guerra, D., Stewart, D., 2018. Sex-determining mechanisms in bivalves. In: Leonard, J. (Ed.), Transitions Between Sexual Systems. Springer, Cham. https://doi.org/10.1007/978-3-319-94139-4_6.

Broquard, C., Martinez, A.S., Maurouard, E., Lamy, J.B., Degremont, L., 2020. Sex determination in the oyster *Crassostrea gigas*——a large longitudinal study of population sex ratios and individual sex changes. Aquaculture 515, 734555. https://doi.org/10.1016/j.aquaculture.2019.734555.

Catchen, J., Hohenlohe, P.A., Bassham, S., Amores, A., Cresko, W.A., 2013. Stacks: an analysis tool set for population genomics. Mol. Ecol. 22, 3124–3140. https://doi.org/10.1111/mec.12354.

Chen, S., Zhou, Y., Chen, Y., Gu, J., 2018. fastp: an ultra-fast all-in-one FASTQ preprocessor. Bioinformatics 34, 884–890. https://doi.org/10.1093/bioinformatics/bty560.

D'Mello, S.A.N., Finlay, G.J., Baguley, B.C., Askarian-Amiri, M.E., 2016. Signaling pathways in melanogenesis. Int. J. Mol. Sci. 17, 1144. https://doi.org/10.3390/ijms17071144.

Elshire, R.J., Glaubitz, J.C., Sun, Q., Poland, J.A., Kawamoto, K., Buckler, E.S., Mitchell, S.E., 2011. A robust, simple genotyping-by-sequencing (GBS) approach for high diversity species. PLoS One 6, e19379. https://doi.org/10.1371/journal.pone.0019379.

Evans, S., Camara, M.D., Langdon, C.J., 2009. Heritability of shell pigmentation in the Pacific oyster, *Crassostrea gigas*. Aquaculture 286, 211–216. https://doi.org/10.1016/j.aquaculture.2008.09.022.

Ge, J.L., Li, Q., Yu, H., Kong, L.F., 2015. Mendelian inheritance of golden shell color in the Pacific oyster *Crassostrea gigas*. Aquaculture 441, 21–24. https://doi.org/10.1016/j.aquaculture.2015.01.031.

Gjedrem, T., Rye, M., 2018. Selection response in fish and shellfish: a review. Rev. Aquac. 10, 168–179. https://doi.org/10.1111/raq.12154.

Guo, X., Li, Q., Wang, Q.Z., Kong, L.F., 2012. Genetic mapping and QTL analysis of growth-related traits in the Pacific oyster. Mar. Biotechnol. 14, 218–226. https://doi.org/10.1007/s10126-011-9405-4.

Guo, X.M., Hedgecock, D., Hershberger, W.K., Cooper, K., Allen, S.K., 1998. Genetic determinants of protandric sex in the Pacific oyster, *Crassostrea gigas* thunberg. Evolution 52, 394–402. https://doi.org/10.2307/2411076.

Han, Z.Q., Li, Q., 2018. Different responses between orange variant and cultured population of the Pacific oyster *Crassostrea gigas* at early life stage to temperature-salinity combinations. Aquac. Res. 49, 2233–2239. https://doi.org/10.1111/are.13680.

Han, Z.Q., Li, Q., 2020. Mendelian inheritance of orange shell color in the Pacific oyster *Crassostrea gigas*. Aquaculture 516, 734616. https://doi.org/10.1016/j.aquaculture.2019.734616.

Han, Z.Q., Li, Q., Liu, S.K., Yu, H., Kong, L.F., 2019. Genetic variability of an orange-shell line of the Pacific oyster *Crassostrea gigas* during artificial selection inferred from microsatellites and mitochondrial COI sequences. Aquaculture 508, 159–166. https://doi.org/10.1016/j.aquaculture.2019.04.074.

Hedgecock, D., Shin, G., Gracey, A.Y., Van Den Berg, D., Samanta, M.P., 2015. Second-generation linkage maps for the Pacific Oyster *Crassostrea gigas* reveal errors in assembly of genome scaffolds. G3 5, 2007–2019. https://doi.org/10.1534/g3.115.019570.

Hedrick, P.W., Hedgecock, D., 2010. Sex determination: genetic models for oysters. J. Hered. 101, 602–611. https://doi.org/10.1093/jhered/esq065.

Hoang, T.H., Stone, D.A.J., Duong, D.N., Bansemer, M.S., Harris, J.O., Qin, J.G., 2017. Colour change of greenlip abalone (*Haliotis laevigata* Donovan) fed formulated diets containing graded levels of dried macroalgae meal. Aquaculture 468, 278–285. https://doi.org/10.1016/j.aquaculture.2016.10.027.

Hu, Z., Song, H., Yang, M.J., Yu, Z.L., Zhou, C., Wang, X.L., Zhang, T., 2019. Transcriptome analysis of shell color-related genes in the hard clam *Mercenaria mercenaria*. Comp. Biochem. Physiol. Part D Genomics Proteomics 31, 100598. https://doi.org/10.1016/j.cbd.2019.100598.

Kurosu, H., Choi, M., Ogawa, Y., Dickson, A.S., Goetz, R., Eliseenkova, A.V., Mohammadi, M., Rosenblatt, K.P., Kliewer, S.A., Kuro-o, M., 2007. Tissue-specific expression of βklotho and fibroblast growth factor (FGF) receptor isoforms determines metabolic activity of FGF19 and FGF21. J. Biol. Chem. 282, 26687–26695. https://doi.org/10.1074/jbc.M704165200.

Laghari, M.Y., Lashari, P., Zhang, Y., Sun, X.W., 2014. Identification of quantitative trait loci (QTLs) in aquaculture species. Rev. Fish. Sci. Aquac. 22, 221–238. https://doi.org/10.1080/23308249.2014.931172.

Li, C., Wang, J., Song, K., Meng, J., Xu, F., Li, L., Zhang, G., 2018. Construction of a high-density genetic map and fine QTL mapping for growth and nutritional traits of *Crassostrea gigas*. BMC Genomics 19, 626. https://doi.org/10.1186/s12864-018-4996-z.

Li, H., Durbin, R., 2009. Fast and accurate short read alignment with Burrows-Wheeler transform. Bioinformatics 25, 1754–1760. https://doi.org/10.1093/bioinformatics/btp324.

Nie, H., Yan, X., Huo, Z., Jiang, L., Chen, P., Liu, H., Ding, J., Yang, F., 2017. Construction of a high-density genetic map and quantitative trait locus mapping in the Manila clam *Ruditapes philippinarum*. Sci. Rep. 7, 229. https://doi.org/10.1038/s41598-017-00246-0.

Sambrook, J., Russell, D.W., 2001. Molecular Cloning: A Laboratory Manual, 3rd ed. Cold Spring Harbor Laboratory Press, Cold Spring Harbor, NY.

Santerre, C., Sourdaine, P., Marc, N., Mingant, C., Robert, R., Martinez, A.S., 2013. Oyster sex determination is influenced by temperature——first clues in spat during first gonadic differentiation and gametogenesis. Comp. Biochem. Physiol. Part A Mol. Integr. Physiol. 165, 61–69. https://doi.org/10.1016/j.cbpa.2013.02.007.

Saternus, R., Pilz, S., Graber, S., Kleber, M., Marz, W., Vogt, T., Reichrath, J., 2015. A closer look at evolution: variants (SNPs) of genes involved in skin pigmentation, including EXOC2, TYR, TYRP1, and DCT, are associated with 25(OH)D serum concentration. Endocrinology 156, 39–47. https://doi.org/10.1210/en.2014-1238.

Schneider, T., Grosbois, G., Vincent, W.F., Rautio, M., 2016. Carotenoid accumulation in copepods is related to lipid metabolism and reproduction rather than to UV-protection. Limnol. Oceanogr. 61, 1201–1213. https://doi.org/10.1002/lno.10283.

Sirianni, R., Chimento, A., Ruggiero, C., De Luca, A., Lappano, R., Ando, S., Maggiolini, M., Pezzi, V., 2008. The novel estrogen receptor, G protein-coupled receptor 30, mediates the proliferative effects induced by 17 beta-estradiol on mouse spermatogonial GC-1 cell line. Endocrinology 149, 5043–5051. https://doi.org/10.1210/en.2007-1593.

Slominski, A.T., Brozyna, A.A., Zmijewski, M.A., Jozwicki, W., Jetten, A.M., Mason, R.S., Tuckey, R.C., Elmets, C.A., 2017. Vitamin D signaling and melanoma: role of vitamin D and its receptors in melanoma progression and management. Lab. Investig. 97, 706–724. https://doi.org/10.1038/labinvest.2017.3.

Sonah, H., Bastien, M., Iquira, E., Tardivel, A., Legare, G., Boyle, B., Normandeau, E., Laroche, J., Larose, S., Jean, M., Belzile, F., 2013. An improved genotyping by sequencing (GBS) approach offering increased versatility and efficiency of SNP discovery and genotyping. PLoS One 8, e54603. https://doi.org/10.1371/journal.pone.0054603.

Song, J., Li, Q., Yu, Y., Wan, S., Han, L., Du, S., 2018. Mapping genetic loci for quantitative traits of golden shell color, mineral element contents, and growth-related traits in Pacific Oyster (*Crassostrea gigas*). Mar. Biotechnol. 20, 666–675. https://doi.org/10.1007/s10126-018-9837-1.

Stenger, P.L., Vidal-Dupior, J., Reisser, C., Planes, S., Ky, C.L., 2019. Colour plasticity in the shells and pearls of animal graft model *Pinctada margaritifera* assessed by HSV colour quantification. Sci. Rep. 9, 7520. https://doi.org/10.1038/s41598-019-43777-4.

Swinkels, B.W., Gould, S.J., Bodnar, A.G., Rachubinski, R.A., Subramani, S., 1991. A novel, cleavable peroxisomal targeting signal at the amino-terminus of the rat 3-ketoacyl-coa thiolase. EMBO J. 10, 3255–3262. https://doi.org/10.1002/j.1460-2075.1991.tb04889.x.

Teng, W., Cong, R.H., Que, H.Y., Zhang, G.F., 2018. De novo transcriptome sequencing reveals candidate genes involved in orange shell coloration of bay scallop *Argopecten irradians*. J. Ocean. Limnol. 36, 1408–1416. https://doi.org/10.1007/s00343-018-7063-3.

Van Ooijen, J.W., 2006. JoinMap® 4.0: Software for the Calculation of Genetic Linkage Maps in Experimental Populations. Kyazma BV, Wageningen, Netherlands.

Van Ooijen, J.W., 2009. MapQTL® 6.0: Sofware for the Mapping of Quantitative Trait Loci in Experimental Populations of Diploid Species. Kyazma BV, Wageningen, Netherlands.

Voorrips, R.E., 2002. MapChart: software for the graphical presentation of linkage maps and QTLs. J. Hered. 93, 77–78. https://doi.org/10.1093/jhered/93.1.77.

Wan, S., Li, Q., Liu, T., Yu, H., Kong, L., 2017. Heritability estimates for shell color-related traits in the golden shell strain of Pacific oyster (*Crassostrea gigas*) using a molecular pedigree. Aquaculture 476, 65–71. https://doi.org/10.1016/j.aquaculture.2017.04.012.

Wang, J., Li, Q., Zhong, X., Song, J., Kong, L., Yu, H., 2018. An integrated genetic map based on EST-SNPs and QTL analysis of shell color traits in Pacific oyster *Crassostrea gigas*. Aquaculture 492, 226–236. https://doi.org/10.1016/j.aquaculture.2018.04.018.

Wang, J.P., Li, L., Zhang, G.F., 2016. A high-density snp genetic linkage map and QTL analysis of growth-related traits in a hybrid family of Oysters (*Crassostrea gigas* x *Crassostrea angulata*) using genotyping-by-sequencing. G3 6, 1417–1426. https://doi.org/10.1534/g3.116.026971.

Williams, S.T., 2017. Molluscan shell colour. Biol. Rev. 92, 1039–1058. https://doi.org/10.1111/brv.12268.

Xu, C., Li, Q., Yu, H., Liu, S., Kong, L., Chong, J., 2019. Inheritance of shell pigmentation in Pacific oyster *Crassostrea gigas*. Aquaculture 512. https://doi.org/10.1016/j.aquaculture.2019.734249.

Xu, L., Li, Q., Yu, H., Kong, L., 2017. Estimates of heritability for growth and Shell color traits and their genetic correlations in the black Shell strain of Pacific oyster *Crassostrea gigas*. Mar. Biotechnol. 19, 421–429. https://doi.org/10.1007/s10126-017-9772-6.

Yasuoka, N., Yusa, Y., 2016. Effects of size and gregariousness on individual sex in a natural population of the Pacific oyster *Crassostrea gigas*. J. Molluscan Stud. 82, 485–491. https://doi.org/10.1093/mollus/eyw020.

Yue, C.Y., Li, Q., Yu, H., 2018. Gonad transcriptome analysis of the Pacific Oyster *Crassostrea gigas* identifies potential genes regulating the sex determination and differentiation process. Mar. Biotechnol. 20, 206–219. https://doi.org/10.1007/s10126-018-9798-4.

Zhang, N., Xu, F., Guo, X.M., 2014. Genomic analysis of the Pacific Oyster (*Crassostrea gigas*) reveals possible conservation of vertebrate sex determination in a mollusc. G3 4, 2207–2217. https://doi.org/10.1534/g3.114.013904.